ARTICLE
Toxicology Communications 2022;4(2):6. https://doi.org/10.53388/2022020206

Prediction of the mechanisms of liver injury of Epimedii Folium by network pharmacology and validation in HepaRG Cells

Xiao-Tong Duan[1], Shan Li[1], Qi-Yi Wang[2], Jing-Xian Liu[1], Tian-Mu He[1], Liu Liu[1], Mei-Chen Liu[1], Yun Liu[1], Rong Yan[1], Jian-Yong Zhang[2,3*], Xiao-Fei Li[1*]

[1]School of Basic Medicine, Zunyi Medical University, Zunyi 563000, China. [2]School of Pharmacy, Zunyi medical university, Zunyi 563000, China. [3]Key Laboratory of Basic Pharmacology Ministry Education and Joint International Research Laboratory of Ethnomedicine Ministry of education, Zunyi Medical University, Zunyi 563000, China.

***Corresponding to:** Jian-Yong Zhang. School of Pharmacy, Zunyi medical university, No.6 West Xuefu Road, Zunyi 563000, China. E-mail: zhangjianyong2006@126.com. Xiao-Fei Li. School of Basic Medicine, Zunyi Medical University, No.6 West Xuefu Road, Zunyi 563000, China. E-mail: Lixiaofei@zmu.edu.cn.

Competing interests
The authors declare no conflicts of interest.

Acknowledgment
This work is supported by the National Natural Science Foundation of China (Grants no. 81760746, 81803838 and 82060754); Science and Technology Department of Guizhou province of China ([2016]2854, [2020]1Y376, [2019]1346, ZK[2021]532, QKH[2019]1346, ZK[2022]615); Innovation talent team of Guizhou science and Technology Department (QKH platform talents[2020]5007); Education Department of Guizhou Province of China (GNYL[2017]006, [2017]078, [2012]311); Science and Technology Department of Zunyi city of Guizhou province of China([2020]7, [2020]39, [2021]3, [2021]532); Science and Technology Department of Honghuagang District of Zunyi city of Guizhou province of China ([2020]17).

Abbreviations
EF, Epimedii Folium; DILI, drug-induced liver injury; HILI, Herbal induced liver injury; TCM, Traditional Chinese medicine; TCMSP, Traditional Chinese Medicine Systems Pharmacology Database; OB, oral bioavailability; DL, drug-likeness; C-T, compound-target; BP, biological processes; T-P, Target-pathway; CC, cellular components; MF, molecular functions; TFE, epimedium flavonoids; GOBP, Gene Ontology Biological Process; GOCC, GO Cellular Component; GOMF, GO Molecular Function; NAFLD, Non-alcoholic fatty liver disease; C-T-P, compound-target-pathway network.

Peer review information
Toxicology Communications thanks Mahmoud Mohamed Elalfy and other anonymous reviewers for their contribution to the peer review of this paper.

Citation
Duan XT, Li S, Wang QY, et al. Prediction of the mechanisms of liver injury of Epimedii Folium by network pharmacology and validation in HepaRG Cells. *Toxicol Commun* 2022;4(2):6. doi: 10.53388/2022020206.

Executive editor: Guang-Ze Ma.
Received: 13 February 2022; **Accepted:** 18 March 2022; **Available online:** 30 March 2022.

Abstract
Objective: Epimedii Folium (EF), a traditional Chinese medicinal material, has the effect of tonifying kidney Yang, strengthening bones and treating rheumatism. However, its clinical applications are limited by its drug-induced liver injury (DILI) effects and the underlying mechanisms have not been elucidated. **Methods:** Active EF compounds were obtained from the TCMSP database and their targets predicted in Targetnet. Next, DILI-targets were obtained from CTD, Genecards and Digsee databases. Protein-protein interactions of EF DILI-targets were determined using STRING and hub targets identified via topological analyses. Then, hub targets were subjected to GO and KEGG pathway enrichment analyses. Finally, HepaRG cells were used for further validation of molecular mechanisms. **Results:** Fifty seven active compounds and 164 targets that interacted with these active compounds were identified with Sagittatoside A, icariside I, and Icariin being the best active compounds. Enrichment analysis revealed the PI3K/Akt and NF-kB signaling pathways to be markedly enriched. Molecular docking revealed that Sagittatoside A, icariside I and Icariin had good binding activities to RAC1, PTGS2, and NOS3. Validation analysis in HepaRG cells revealed that Epimedium flavonoids upregulated RAC1, PTGS2 and NOS3 levels. **Conclusion:** Our findings show that EF induces oxidative stress, inflammation, and apoptosis via PI3K/Akt and NF-kB signaling pathways, and provides a basis for more in-depth studies on EF-induced DILI.

Keywords: Epimedii Folium; drug-induced liver injury; network pharmacology; experimental validation; molecular mechanism

Introduction

Drug-induced liver injury (DILI), which may result from the drug itself or its metabolites, results in hepatocyte necrosis and liver damage through severe oxidative stress, inflammation and apoptosis [1–4]. Clinically, DILI accounts for 10–15% of drug adverse reactions, and more than 1,000 drugs are potential for DILI [5–8]. Herbal induced liver injury (HILI) is a type of DILI that is attributed to Chinese herbal medicines and accounts for about 20% of all DILI cases [9]. Due to global applications of Traditional Chinese medicine (TCM), liver injuries from TCMs are of significance [10].

Epimedii Folium (EF), a classical Yang-tonifying and bone-strengthening medicine, is commonly used in TCM. Flavonoids are the main active compounds in EF, and they exhibit various effects, including anti-inflammatory, immune regulation, antioxidant, and anti-tumor effects [11]. Various TCM compounds, such as Xianling Gubao Capsule and Zhuanggujian Pill that contain EF have been associated with significant DILI, and EF is a cause of DILI [12–19]. EF inhibits normal hepatocyte metabolism, causes capillary bile duct cholestasis and damages liver functions [20, 21]. Moreover, EF induces inflammatory responses and activates oxidative stress [22]. However, due to the complexity of EF compounds, the mechanisms involved in EF-induced DILI have not been fully elucidated.

Network pharmacology is a systematic method that is based on disease, target, and drug interactions. This system-based research method is similar to the holistic regulation effect of TCMs and is widely used in studying the pharmacological and toxicological mechanisms of TCM [23–26]. However, findings from network prediction should be experimentally validated. For instance, a study using network pharmacology and a zebrafish model found that > 22 active ingredients of *Cistanche tubulosa*, which is used to treat osteoporosis and Alzheimer's Disease, regulate NF-kB and MAPK signaling pathways. Therefore, a combination of network pharmacology and experimental verification can better elucidate on the toxicological mechanisms of EF.

Thus, network pharmacology combined with molecular docking were used to analyze the active compounds, drug targets and key pathways of EF-associated DILI. Finally, key targets were validated in HepaRG cells. Our findings form the basis for further studies on EF-induced DILI. The workflow of this study is shown in Figure 1.

Materials and methods

Network pharmacology study

Screening of active compounds in EF All EF chemical compounds were obtained from the Traditional Chinese Medicine Systems Pharmacology Database (TCMSP, http://lsp.nwu.edu.cn/tcmsp.php) and published studies. Two ADME models, including oral bioavailability (OB) and drug-likeness (DL) models were used to predict the potential active compounds. Based on the drug screening standard recommended by TCMSP, active EF compounds were indicated by oral bioavailability (OB) ≥ 20% and drug-likeness (DL) of ≥ 0.10.

Identification of active compound targets and network construction Targetnet (http://targetnet.scbdd.com/) was used to identify the targets for active EF compounds. Then, EF-targets and EF active compounds were input into Cytoscape 3.7.0 and a compound-target (C-T) network constructed to determine potential interactions between EF-targets and active EF compounds.

Potential disease targets for DILI The DILI-related target genes were identified from GeneCards (http://www.genecards.org/), CTD (http://ctdbase.org/), and Digsee (http://www.geneSearch/) by searching for various keywords: “liver injury”, “liver toxicity”, “hepatotoxicity” or “hepatic toxicity”. Only “Homo sapiens” results were selected as DILI-related targets. Targets at the intersections of DILI-related targets and predicted EF-targets were selected as EF DILI-targets.

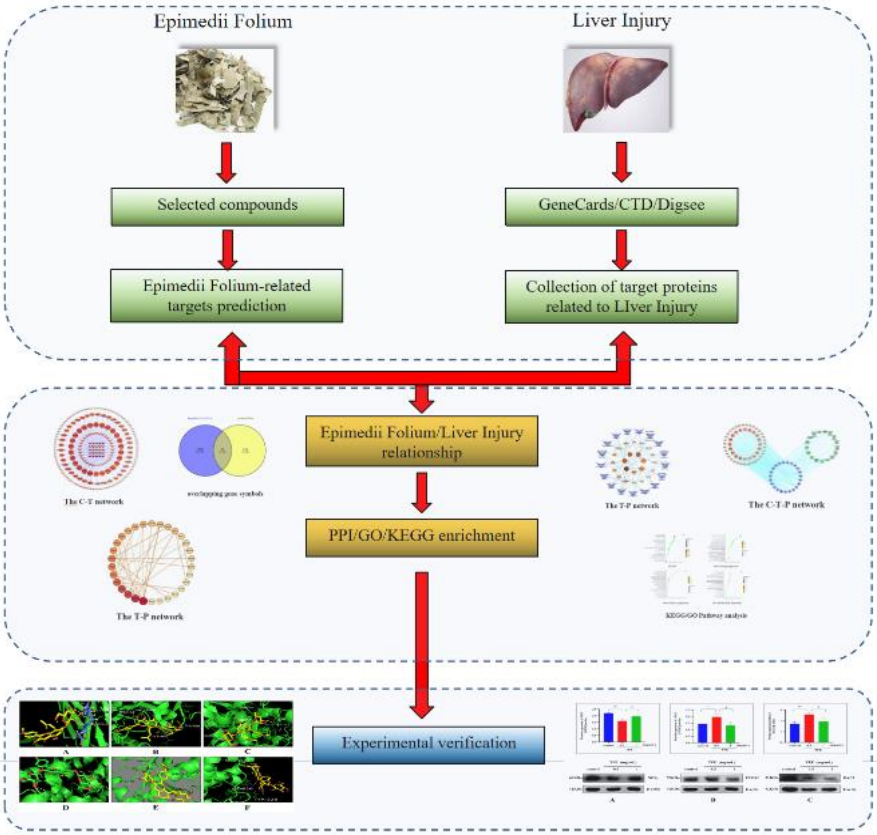

Figure 1 Research workflow diagram of EF-indcued DILI

Construction of the protein-protein interaction (PPI) network Next, STRING (http://string.org/) was used to construct a PPI network of EF DILI-targets and targets with confidence scores >0.7 selected. Finally, hub targets of EF and active compounds were identified by values of degree and betweenness for constructing a compound- target network.

GO and KEGG pathway enrichment analyses GO analysis consisted of biological processes (BP), cellular components (CC), and molecular functions (MF). KEGG pathway analysis provides important information on the mechanisms of a certain drug on a disease. In this study, GO and KEGG pathway enrichment analyses were performed on hub EF targets using Enrichr (https://maayanlab.cloud/). $P \leq 0.05$ indicated significant enrich-ments.

Molecular docking analysis Molecular docking is a process involving the docking of small ligands (active compounds) with proteins (hub targets) for scoring its complementary values at binding sites using the iGEMDOCK 2.1 software. First, the top-8 active compounds in the CTP network were downloaded from Pubchem (https://pubchem.ncbi.nlm.nih.gov), their energy minimized via Chem3D 19.0 software and saved in mol format. Target proteins were downloaded from PDB (http://www.rcsb.org/). Energies of the top-8 targets in the T-P network and active compounds were assessed by the iGEMDOCK software. Standard docking settings in iGEMDOCK were: population size = 200, generations = 70, and number of solutions = 2. Lower energies correlated with more stable constructions.

Experimental verification

Cell cultures HepaRG cells (Chinese Academy of Sciences Cell Bank) were grown in RPMI 1640 medium (Gibco, USA) supplemented with 10% FBS (Gibco, USA), 1% pens/strep (100 U/mL penicillin and 100 μg/mL streptomycin) and 50 μM hydrocortisone (Solarbio, China) in a humified incubator at 37 ℃ in a 5% CO_2 atmosphere.

Preparation of epimedium flavonoids (TFE) TFE (Purity:50%, Chengdu Mingrui Technology Co. Ltd) was dissolved in DMSO (Solarbio, China) and stored at -20℃. Prior to use, it was diluted to the desired concentrations using a complete medium.

Cell proliferation assays Single cell suspensions of HepaRG cells were prepared at 1×105 cells/mL and seeded in 96-well plates at 100 μL per well, and incubated for 24h at 37℃, 5% CO_2. After pre-treatments with TFE at 0.0625, 0.125, 0.25, 0.5, and 1 mg/mL for 12 h, the media was replaced with 100 μL 10% CCK-8 medium solution. Then, cells were incubated under normal conditions for 2 h and absorbance read at 450 nm using a Bio Tek microplate reader (VT 05404-0998).

Evaluation of cell apoptosis by Hoechst staining HepaRG cells were assigned into a control and TFE group, seeded in a 6-well plate at 1.4×10^5 cells/mL, treated with 1 mg/mL TFE for 12 h, washed twice using PBS 1X, fixed for 15 min in precooled 4% PFA after which 10 μL of Hoechst 33342 (100×) was then added to each well for 25 min and apoptosis evaluated by inverted fluorescence microscopy.

Western blot analysis Cells were treated with TFE at 0.5 or 1 mg/mL for 12 h followed by protein extractions. Western blot analysis was used to assess RAC1, PTGS2 and NOS3 protein levels. Briefly, proteins were resolved by 10% polyacrylamide gel electrophoresis, transferred to PVDF membranes, and blocked for 1 h using 5% milk. The PVDF membranes were immersed in a tube containing 6 mL antibody solutions for RAC1, PTGS2, and NOS3 (Cell signaling technology, all at 1:1,000) and incubated overnight at 4 ℃. After washing thrice using the TBST buffer, blots were incubated for 2 h at room temperature in the presence of a secondary antibody (dilution ratio: 1:3,000). Finally, proteins were visualized using an ECL imaging agent and a chemometric gel imaging system. The Image Lab (Bio-Rad, Version 3.0) software was used to analyze gray levels of the proteins.

Statistical analysis Data are expressed as means ± SD for n = 3. GraphPad prism 8.0 was used for statistical analyses. Comparisons of means among multiple groups was performed by one-way ANOVA. $P \leq 0.05$ was the threshold for statistical significance.

Results

Network pharmacology-based study

Screening of active compounds in EF A total of 130 EF compounds were retrieved from TCMSP and 44 active compounds selected based on the OB ≥ 20 and DL ≥ 0.10 criteria. Some compounds, including Icariside, Ikarisoside A, Hyperoside, Epimedin A1, Epimedin B, Epimedin C, Magnoflorine, Cryptochlorogenic Acid, Chlorogenic Acid, Neochlorogenic Acid, Sagittatoside A, Sagittatoside B and 2"-O-Rhamnosylicariside II that did not meet the screening criteria were selected as they are reported to exhibit pharmacological activities (Table 1).

Targets prediction of EF Targets for 57 active compounds were identified using Targetnet and 164 targets of compounds obtained from Uniprot. Finally, a C-T network, which had a total of 221 nodes including 57 compounds, 164 EF-targets and an average degree of 13.3, was constructed using Cytoscape 3.7.0 (Figure 2). Ranked by degree, the top-5 compounds in the network were: EF5 (isoliquiritigenin, degree = 60), EF39 (luteolin, degree = 58), EF14 (Flavone der, degree = 57), EF44 (quercetin, degree = 55) and EF19 (kaempferol, degree = 53). The top-5 targets were: ABCG2 (degree = 40), PTGS2 (degree = 37), ALOX15 (degree = 36), CYP1A2 (degree = 35) and CA6 (degree = 35).

Liver injury targets The 1438 DILI related targets were obtained from CTD, Genecards, and Digsee. Venn diagram intersection analysis of the 1438 DILI related targets and 164 EF-target genes identified 49 EF DILI-targets (Figure 3).

Analyses of the PPI network To study the mechanisms through which EF induces DILI, 49 EF DILI-targets were subjected to STRING (https://string-db.org/) analysis. The average degree was 3.9, node sizes and colors reflected the number of combined targets degree (Figure 4). After removing individual targets, the top-30 hub target genes with higher connections were visualized, including inflammation-associated genes (RAC1, NOS3, PTGS2, MMP9 and HSP90AA1), apoptosis-related genes (CASP9, GSK3B and ICAM1), hormone-related genes (ESR1, AR and PGR), metabolism-related genes (CYP1A2, CYP2C19, MAOA, MAOB and ALOX5) and transcription factor (RELA).

GO and KEGG enrichments The 30 hub target genes were subjected to enrichment analysis using Enrichr. GO analysis identified 472 enriched biological processes, 74 enriched molecular functions and 14 enriched cell components. Gene Ontology Biological Process (GOBP) analysis to verify the EF DILI-targets revealed the top-10 enriched GOBP entries (Figure 5B). We inferred that many biological processes, including monoterpenoid metabolic processes, dopamine catabolic processes, terpenoid metabolic processes, catecholamine catabolic processes, and steroid catabolic processes were closely associated with EF-induced DILI. GO Cellular Component (GOCC) analysis of the roles of EF DILI-targets at the cell level revealed the top-10 entries. Among them, early phagosome, endocytic vesicle lumen, endolysosome membrane, endolysosome and transcriptionally active chromatin were associated with EF induction of DILI (Figure 5C). GO Molecular Function (GOMF) analysis showed that primary amine oxidase activities, arginine binding, NADPH-hemoprotein reductase activities, RNA polymerase II basal transcription factor binding and transcription coactivator binding had important molecular functions in EF induction of DILI. KEGG pathway annotation analysis of signaling pathways involved in EF-induced DILI revealed 97 enriched pathways. After excluding pathways that were unrelated to LI, 17 significant pathways remained (Figure 5A). Target-pathway (T-P) network construction on Cytoscape (Figure 6) revealed that EF DILI-targets were highly clustered in signaling pathways, “VEGF signaling pathway”, “Steroid hormone biosynthesis”, “IL-17 signaling pathway”, “NF-kB signaling pathway” and “PI3K/Akt signaling pathway”, suggesting that inflammatory responses may have important effects on EF-induced DILI.

Compound-target-pathway network model of EF Core compounds in compound-target-pathway network (C-T-P) may modulate the 17 signal pathways by acting on 23 core targets (Table 2, Figure 7), reflecting the characteristics of DILI induced by the multi-compounds,

Table 1 Basic information of the active compounds in EF (Epimedii Folium)

Number	Mol ID	Molecule Name	Pubchem ID	OB (%)	DL
EF1	Mol001510	24-epicampesterol	5283637	37.58	0.71
EF2	Mol001600	copaene	12303902	29.47	0.12
EF3	Mol001645	Linoleyl acetate	5319042	42.1	0.2
EF4	Mol001771	poriferast-5-en-3beta-ol	457801	36.91	0.75
EF5	Mol001789	isoliquiritigenin	638278	85.32	0.15
EF6	Mol001792	DFV	114829	32.76	0.18
EF7	Mol002083	tricin	5281702	27.86	0.34
EF8	MOL002307	20-Hexadecanoylingenol	5318035	28.2	0.68
EF9	Mol002509	Ginkgetin	5271805	22.19	0.59
EF10	Mol002511	Isoginkgetin	5318569	21.56	0.58
EF11	Mol000263	oleanolic acid	10494	29.02	0.76
EF12	Mol002697	junipene	5489258	44.07	0.11
EF13	Mol003044	Chryseriol	5280666	35.85	0.27
EF14	Mol003097	Flavone der.	5281601	27.12	0.27
EF15	Mol000325	(2R,3R)-2-(3,4-dimethoxyphenyl)-7-methoxy-3-methyl-5-[(E)-prop-1-enyl]-2,3-dihydrobenzofuran	6441048	24.19	0.35
EF16	Mol003542	8-Isopentenyl-kaempferol	5318624	38.04	0.39
EF17	Mol000357	Sitogluside	5742590	20.63	0.62
EF18	Mol000359	sitosterol	12303645	36.91	0.75
EF19	Mol000422	kaempferol	5280863	41.88	0.24
EF20	Mol004367	olivil	5273570	62.23	0.41
EF21	Mol004373	Anhydroicaritin	5318980	45.41	0.44
EF22	Mol004379	wushanicariin_qt	3082728	23.36	0.46
EF23	Mol004380	C-Homoerythrinan, 1,6-didehydro-3,15,16-trimethoxy-, (3.beta.)-	296195	39.14	0.49
EF24	Mol004381	Besigomsin	3001662	28.52	0.78
EF25	Mol004382	Yinyanghuo A	5315393	56.96	0.77
EF26	Mol004384	Yinyanghuo C	5315395	45.67	0.5
EF27	Mol004386	Yinyanghuo E	5315397	51.63	0.55
EF28	Mol004388	6-hydroxy-11,12-dimethoxy-2,2-dimethyl-1,8-dioxo-2,3,4,8-tetrahydro-1H-isochromeno[3,4-h]isoquinolin-2-ium	12115137	60.64	0.66
EF29	Mol004391	8-(3-methylbut-2-enyl)-2-phenyl-chromone	17861868	48.54	0.25
EF30	Mol004393	anhydroicaritin	14583584	28.27	0.59
EF31	Mol004394	Anhydroicaritin-3-O-alpha-L-rhamnoside	97041887	41.58	0.61
EF32	Mol004396	1,2-bis(4-hydroxy-3-methoxyphenyl)propan-1,3-diol	12468616	52.31	0.22
EF33	Mol004404	caohuoside D	44259082	24.89	0.83
EF34	Mol004425	Icariin	5318997	41.58	0.61
EF35	Mol004427	Icariside A7	5318401	31.91	0.86
EF36	Mol004428	3,4,6-trimethoxyphenanthrene-2,7-diol	356766	24.46	0.3
EF37	Mol004430	icariside I	5745470	21.88	0.85
EF38	Mol000472	emodin	3220	24.4	0.24
EF39	Mol000006	luteolin	5280445	36.16	0.25
EF40	Mol000622	Magnograndiolide	5319198	63.71	0.19
EF41	Mol000695	patchouli alcohol	10955174	101.96	0.14
EF42	Mol000740	(+)-Cycloolivil	5316262	24.5	0.42
EF43	Mol000008	apigenin	5280443	23.06	0.21
EF44	Mol000098	quercetin	5280343	46.43	0.28
EF45		Icariside II	5488822	3.7	0.84
EF46		Ikarisoside A	5481982	/	/
EF47		Hyperoside	5281643	/	/
EF48		Epimedin A1	92043273	/	/
EF49		Epimedin B	5748393	8.65	0.34
EF50		Epimedin C	5317090	16.29	0.34
EF51		Magnoflorine	73337	0.48	0.55
EF52		Cryptochlorogenic Acid	9798666	/	/
EF53		Chlorogenic Acid	1794427	/	/
EF54		Neochlorogenic Acid	5280633	/	/
EF55		Sagittatoside A	13916054	8.5	0.57
EF56		Sagittatoside B	10146160	5.58	0.64
EF57		2''-O-Rhamnosylicariside II	5318987	/	/

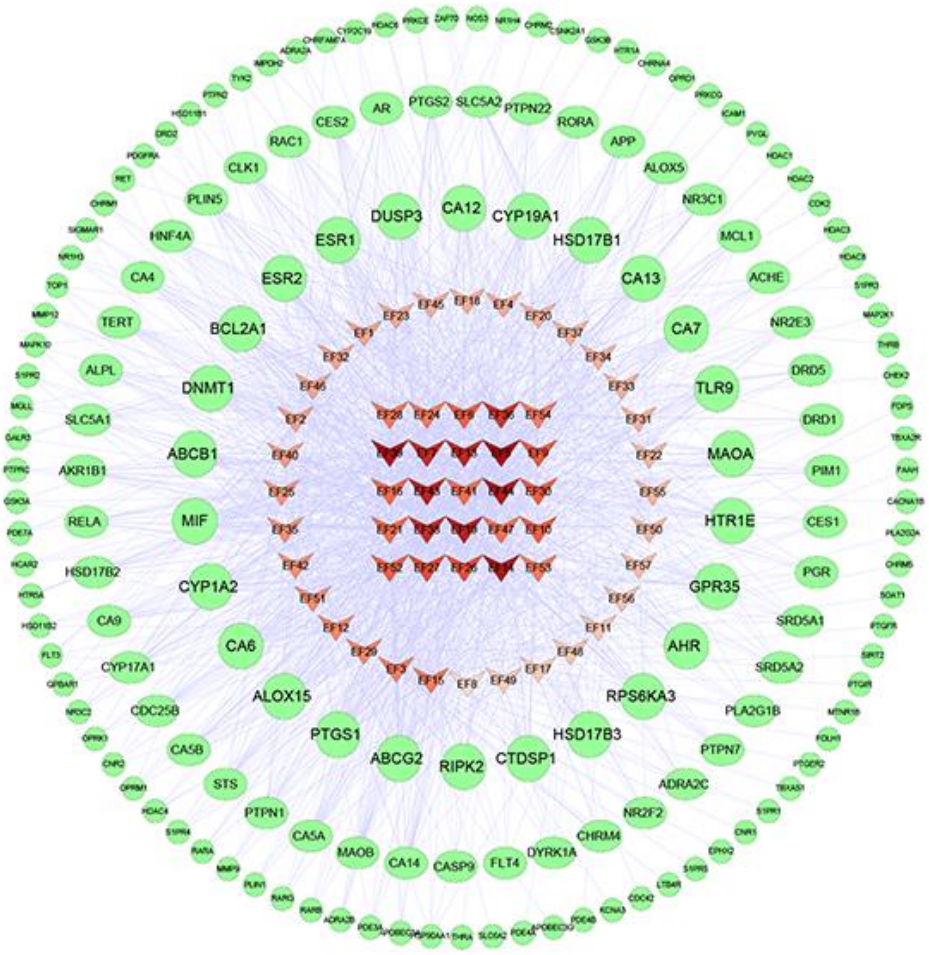

Figure 2 C-T network of EF. The green circle node represents the action targets, the red inverted triangle node represents the active compounds, and the purple line represents the interaction relationship.

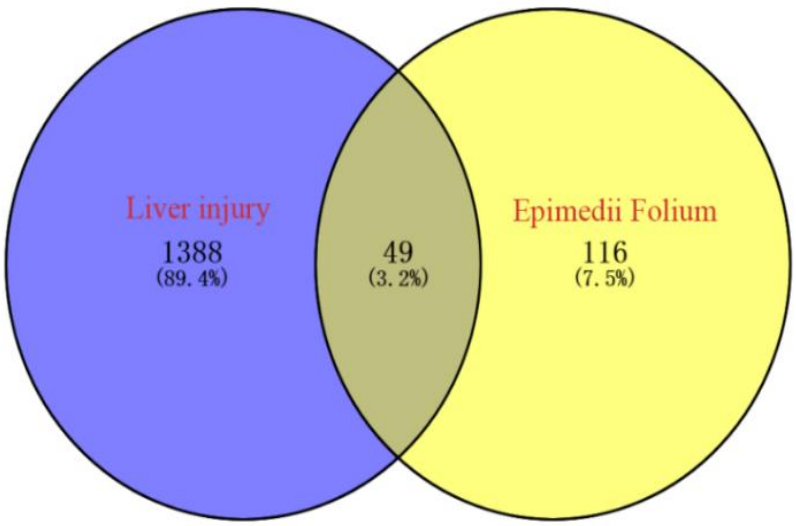

Figure 3 Active target genes of EF inducing on DILI

Toxicology Communications 2022;4(2):6. https://doi.org/10.53388/2022020206

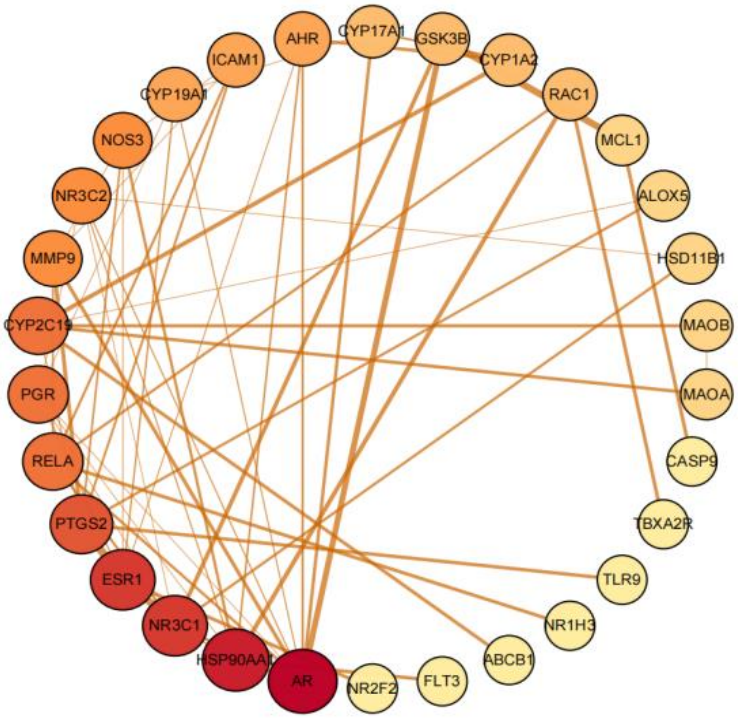

Figure 4 The PPI network of EF-inducd DILI

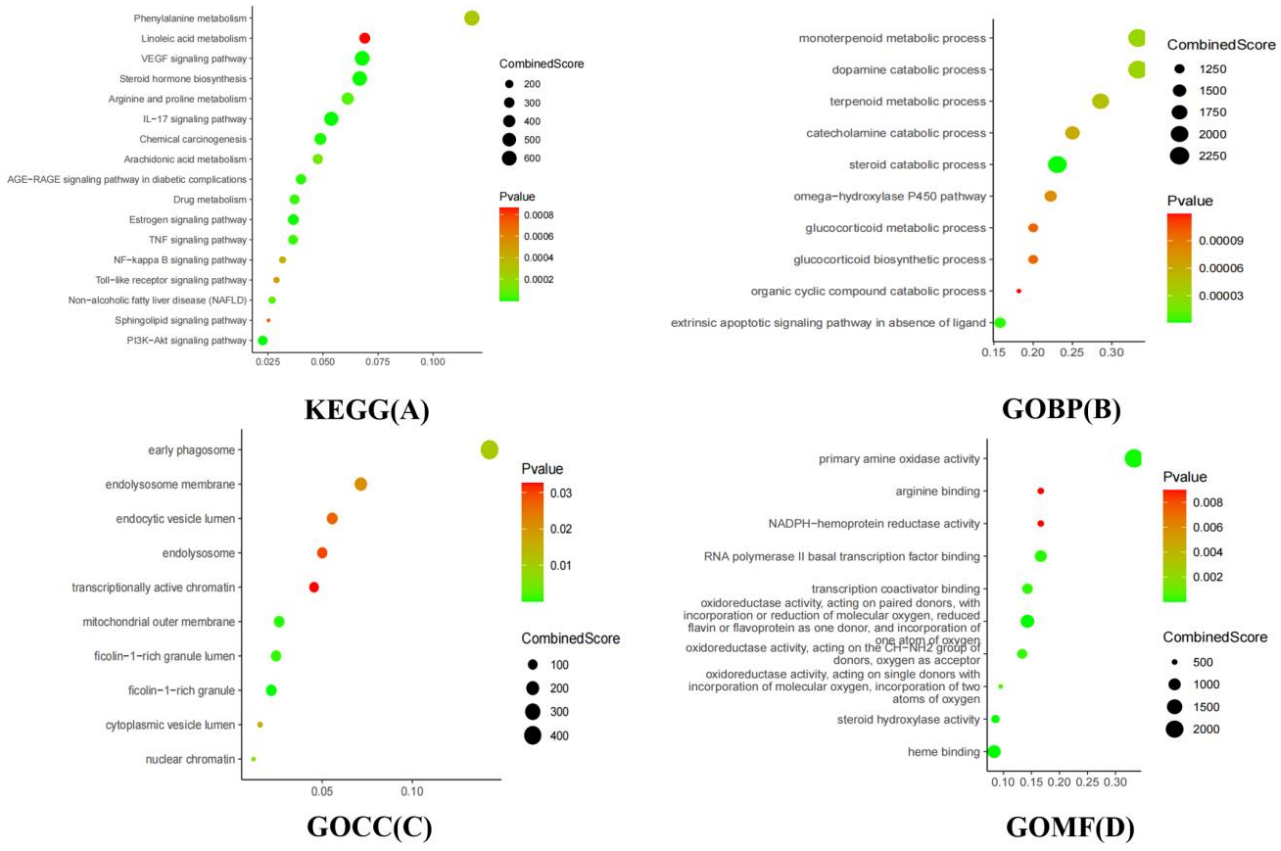

Figure 5 GO and KEGG enrichment analysis results in the lead to EF-inducd DILI

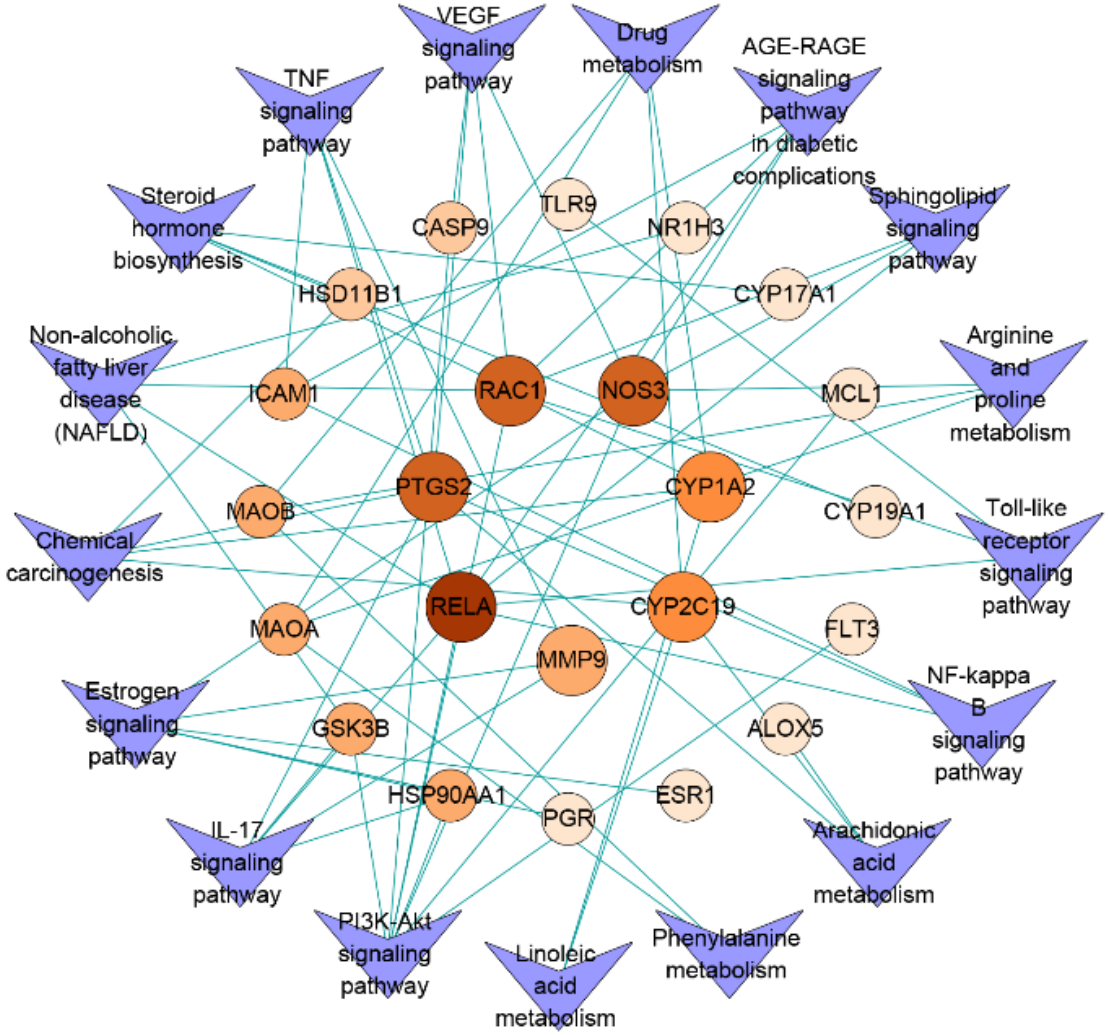

Figure 6 T-P network of EF. The orange circle node represents the hub targets, the purple inverted triangle node represents the pathways, and the green line represents the interaction relationship.

multi-targets, and EF multi-pathway integrations.

Molecular docking analysis Eight hub targets were selected for molecular docking analysis with active compounds. Active site parameters for each target were calculated (Figure 8). Lower docking affinities reflects stronger binding abilities between compounds and their targets, and the binding pose with the strongest affinity was selected to assess interactions between compounds and their targets. The targets that presented the most stable structures were: PTGS2 (-135.311), CYP1A2 (-174.377), ESR1 (-130.25), MMP9 (-165.397), RAC1 (-150.116) and NOS3 (-165.397), indicating that they interact with high-degree compounds (Figure 9).

Experimental verification

Effects of TFE on HepaRG cell proliferations Compared to the control group, HepaRG cell activities for 0.25 mg/mL, 0.5 mg/mL and 1 mg/mL TFE groups were significantly dose-dependently decreased ($P < 0.05$) (Figure 10). Therefore, 0.5 mg/mL and 1 mg/mL TFE were used for subsequent western bolt assays.

Effects of TFE on HepaRG cell morphologies Morphological variations were seen in TFE-treated cells, relative to controls. Control cells (Figure 11A) were evenly distributed at a moderate density. Cell morphologies were spindle-shaped and cells were translucent, with a uniform texture. The morphologies of cells treated with 0.0625 mg/mL TFE (Figure 11B) were similar to those of the control group while cells treated with 0.5 mg/mL TFE (Figure 11C) appeared round and exfoliated. Cells treated with 1 mg/mL TFE (Figure 11D) appeared bubbled, with asymmetrical membranes, and high cell death.

Cell apoptosis assessment by Hoechst staining There were differences in cell apoptosis between the TFE group and control groups. The nuclei of control cells were normal blue, while those of cells treated with 1 mg/mL TFE were bright blue and densely stained, indicating that TFE induced HepaRG apoptosis (Figure 12).

Protein expressions in HepaRG cells treated with TFE The T-P network analysis revealed the top-5 targets to be RELA, PTGS2, RAC1, NOS3 and CYP1A2. Enrichment analysis and literature indicated that RAC1, PTGS2 and NOS3 are involved in PI3K/Akt and NF-kB signaling, which influences inflammation and apoptosis. To validate this finding, we analyzed RAC1, PTGS2, and NOS3 levels by Western blot and observed that relative to control cells, treating HepaRG cells with TFE for 12 h up-regulated PTGS2 (Figure 13B) and RAC1 (Figure 13C) protein levels, while NOS3 (Figure 13A) levels were suppressed and then increased ($^{*}P \leqslant 0.05$ or $^{**}P \leqslant 0.01$). Compared with TFE (0.5 mg/mL) treated cells, protein levels of PTGS2, RAC1 and NOS3were significantly increased in 1 mg/mL TFE treated cells ($^{\#}P < 0.05$ or $^{\#\#}P < 0.01$).

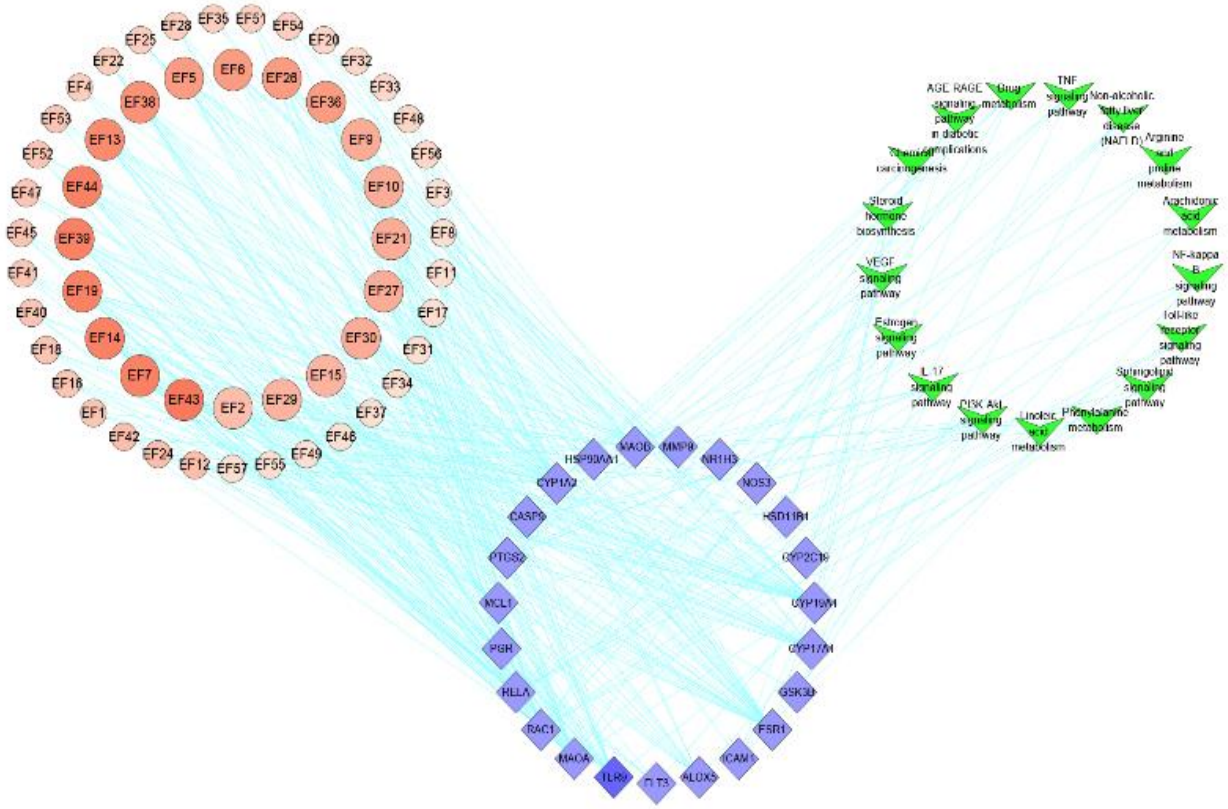

Figure 7 The C-T-P network. The red circular represents compounds, the purple square represents targets, and the green inverted triangle represent, and the bule line represents the interaction relationship.

Table 2 KEGG Pathway Enrichments

Term	Target
PI3K/Akt signaling pathway	CASP9; GSK3B; HSP90AA1; FLT3; NOS3; RAC1; RELA; MCL1
Estrogen signaling pathway	HSP90AA1; NOS3; PGR; ESR1; MMP9
IL-17 signaling pathway	GSK3B; HSP90AA1; PTGS2; MMP9; RELA
Non-alcoholic fatty liver disease (NAFLD)	GSK3B; NR1H3; RAC1; RELA
TNF signaling pathway	PTGS2; MMP9; RELA; ICAM1
Drug metabolism	MAOB; MAOA; CYP1A2; CYP2C19
AGE-RAGE signaling pathway in diabetic complications	NOS3; RAC1; RELA; ICAM1
Chemical carcinogenesis	HSD11B1; CYP1A2; CYP2C19; PTGS2
Steroid hormone biosynthesis	HSD11B1; CYP1A2; CYP19A1; CYP17A1
VEGF signaling pathway	CASP9; NOS3; RAC1; PTGS2
Sphingolipid signaling pathway	NOS3; RAC1; RELA
Toll-like receptor signaling pathway	TLR9; RAC1; RELA
NF-kB signaling pathway	PTGS2; RELA; ICAM1
Arachidonic acid metabolism	ALOX5; CYP2C19; PTGS2
Arginine and proline metabolism	MAOB; MAOA; NOS3
Linoleic acid metabolism	CYP1A2; CYP2C19
Phenylalanine metabolism	MAOB; MAOA

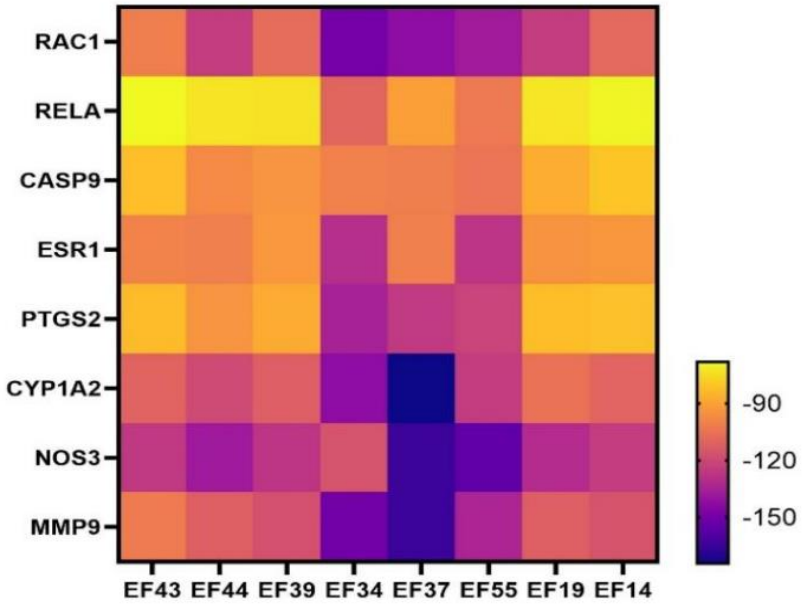

Figure 8 The cluster heat map of molecular docking between compounds and core genes

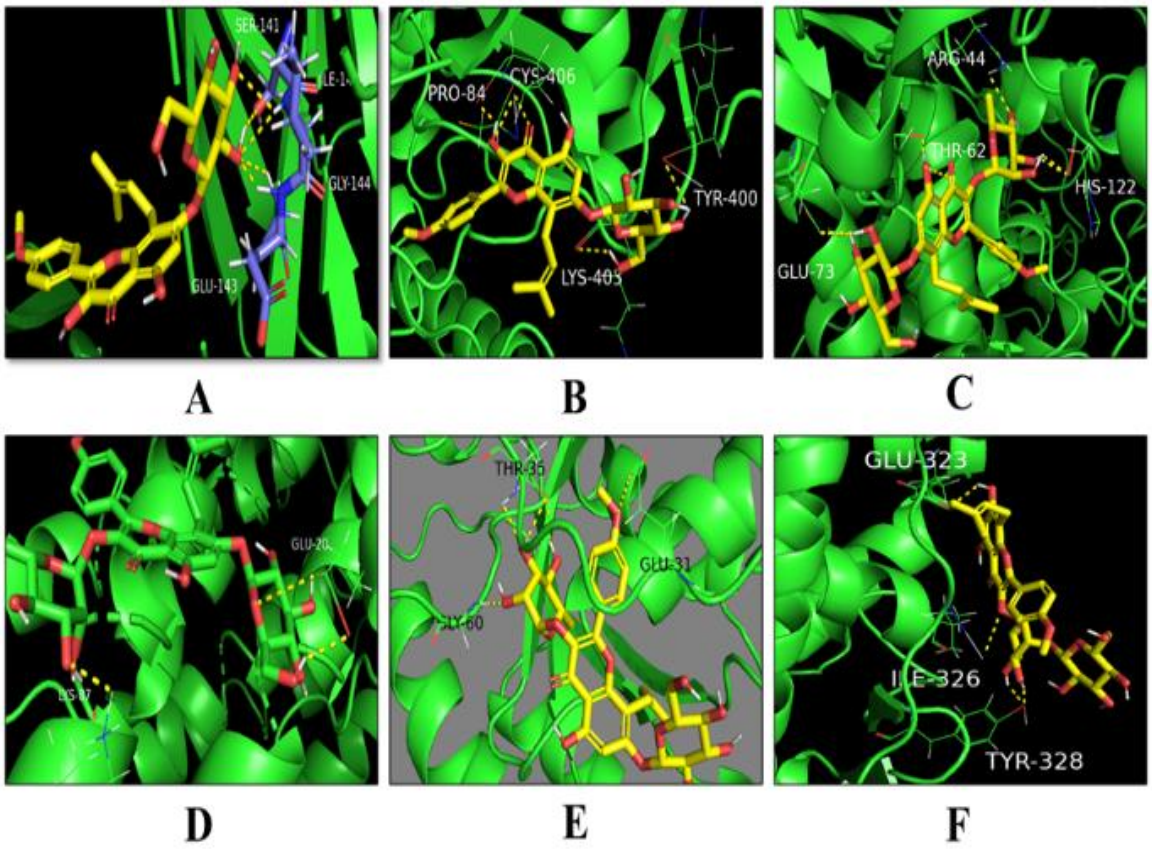

Figure 9 Molecular docking of the targets with the active compounds of EF. (A) Molecular docking model of the icariside I and NOS3; (B) Molecular docking model of the icariside I and CYP1A2; (C) Molecular docking model of the Icariin and PTGS2; (D) Molecular docking model of the Icariin and RELA; (E) Molecular docking model of the Icariin and RAC1; (F) Molecular docking model of the Sagittatoside A and ESR1.

Toxicology Communications 2022;4(2):6. https://doi.org/10.53388/2022020206

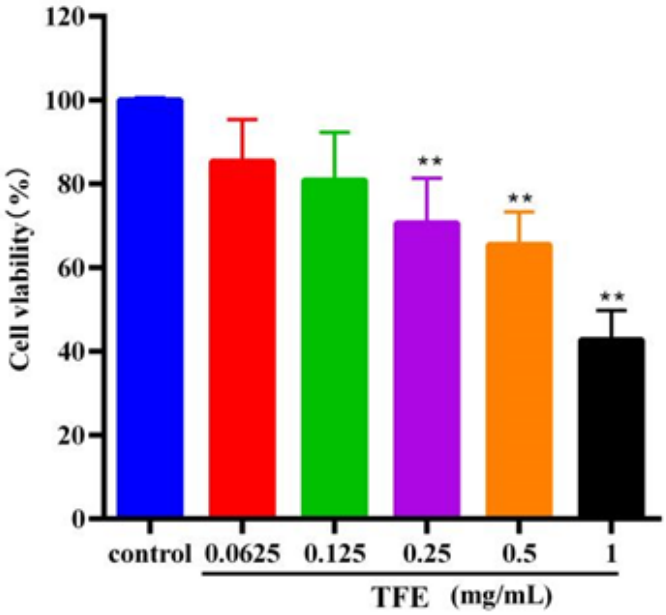

Figure 10 Inhibitory effects of TFE on proliferation of HepaRG cell in 12 h. Results are presented as the x ± s, n = 3. Compared with the control, ** $P < 0.01$.

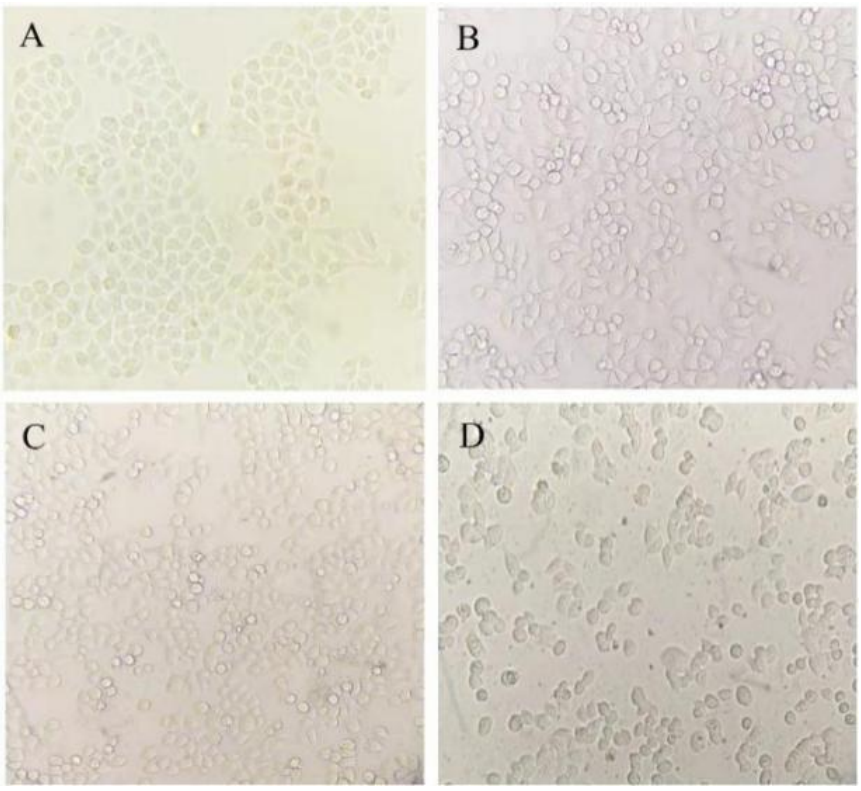

Figure 11 Morphological changes in HepaRG cells treated with different concentrations of TFE (x200). A: control group; B: 0.0625 mg/mL TFE; C: 0.25 mg/mL TFE; D: 0.5 mg/mL TFE

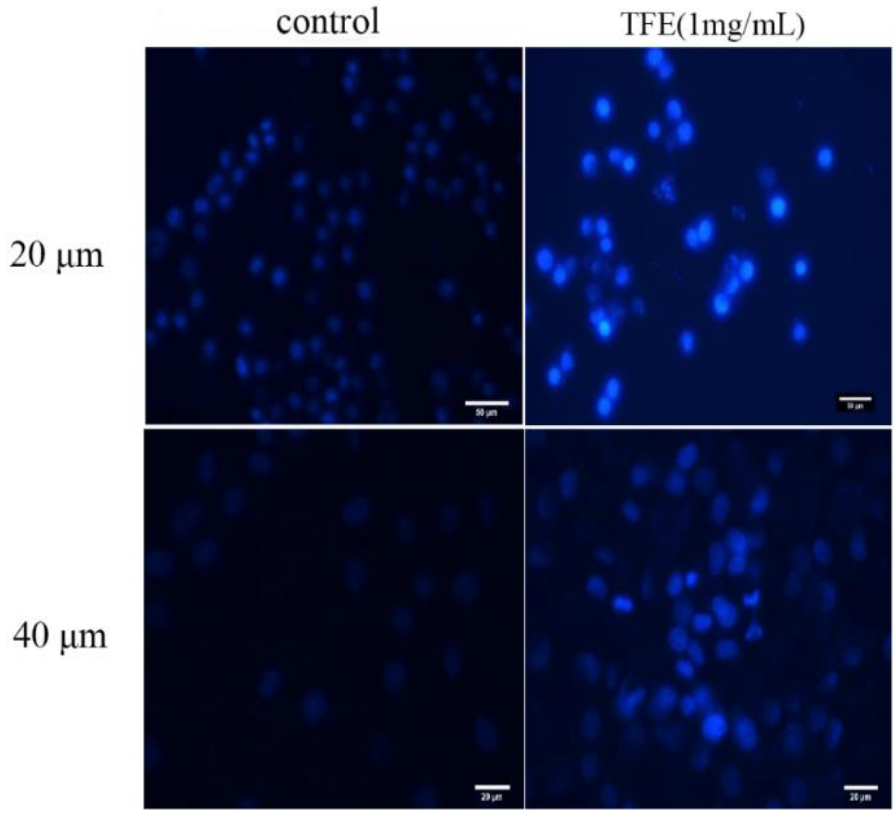

Figure 12 HepaRG cells treated with TFE for 12 hours and stained with Hoechst

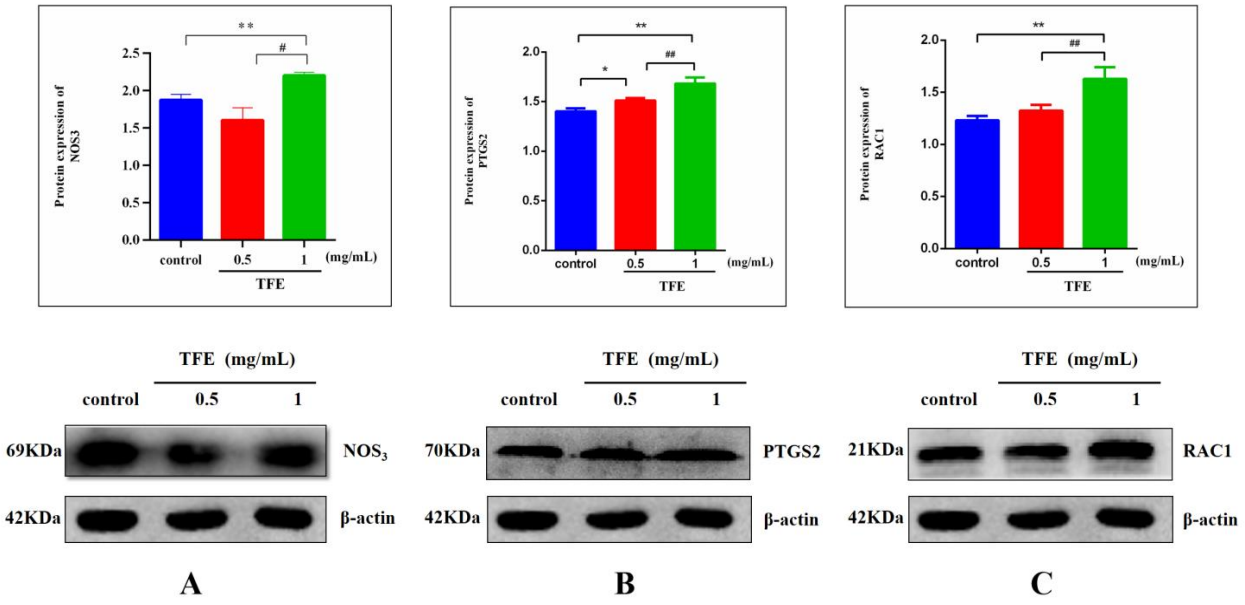

Figure 13 Protein expressions of NOS3, PTGS2 and RAC1 in HepaRG cells. Results are presented as the x ± s, n = 3. Compared with the control $^{*}P < 0.05$ or $^{**}P < 0.01$, and compared with 0.5 mg/mL TFE group $^{\#}P < 0.05$ or $^{\#\#}P < 0.01$.

Discussion

Through network pharmacology, molecular docking, and cell experiments, we elucidated on the mechanisms underlying EF-induced DILI. EF is comprised of various chemical compounds, including flavonoid glycosides and volatile oils. Flavonoid glycosides are the main active ingredients and are regarded as toxic compounds for DILI [27, 28]. Clinically, DILI is the most reported adverse event for EF [18].

In this study, 57 active EF compounds that may act on 23 targets to influence 17 related signaling pathways were identified. GO and KEGG analyses suggested that EF regulates immune pathways and substance metabolism [30–32]. Further experiments showed that EF regulates the expressions of RAC1, PTGS2 and NOS3 and influences PI3K-Akt as well as NF-kB signaling (Figure 14), consistent with network pharmacological results and provides a scientific basis for the potential DILI mechanism of EF [29].

Core compounds of EF

EF-associated DILI has not been conclusively investigated. In this study, the C-T-P network indicated that apigenin, quercetin, luteolin, Sagittatoside A, Icariin, and icariside I are important compounds in EF-induced DILI [33, 34]. Icarisid I, Sagittatoside A and Icariin upregulated ALT, AST, and LDH levels in HL-7702 and HepG2 cells, indicating the disruption of cell membrane integrity and that these compounds may be key in EF-induced DILI [35]. Icariside II contributes to EF-induced DILI by enhancing NLRP3 inflammasome activations.

Icarisid I, Icariside II, Sagittatoside A and Icariin are major TFE compounds. We established that HepaRG cells were dose- dependently damaged by TFE treatment.

Verification of DILI-targets for EF

T-P network analysis revealed important EF targets in DILI to be RAC1, PTGS2, and NOS3. PTGS2 is an important inflammatory factor that is overexpressed in patients with DILI, promoting angiogenesis and inflammation [36, 37]. PTGS2 overexpression promotes tumor growth via VEGF signaling. In NF-kB signaling and molecular docking results, PTGS2 exhibited good binding (-135.311) to Icariin. Further, TFE enhanced PTGS2 expressions in HepaRG cells, indicating that TFE promotes DILI by upregulating PTGS2 expressions, inducing inflammation.

RAC1 is involved in cytoskeleton reorganization and its overexpression induces hepatocyte inflammation via NF-kB signaling [38]. Moreover, RAC1 contributes to necrotic and apoptotic cell death in post-ischemic liver tissues by activating DNA-binding via NF-kB. We found that RAC1 modulates 5 pathways, including PI3K-Akt signaling. Molecular docking revealed that it has good binding (-150.116) effects to Icariin. TFE elevated RAC1 levels in HepaRG cells, indicating that it may drive DILI via RAC1-mediated apoptosis and inflammation.

NO synthesis is catalyzed by nitric oxide synthase (NOS), including the isoforms NOS1, NOS2, and NOS3. NOS3 upregulation destabilize sNOS production, resulting in vascular endothelial dysfunctions. Elevated NOS3 levels in brains of diabetic rats aggravated cell damage by enhancing oxidative stress levels. We found that TEF upregulates NOS3 in HepRG cells, indicating that EF may drive DILI by activating oxidative stress responses and apoptosis via NOS3 upregulation [39].

In summary, RAC1, PTGS2, and NOS3 may be key mediators of EF-driven DILI through modulation of oxidative stress, inflammation, and apoptosis via PI3K-Akt and NF-kB signaling.

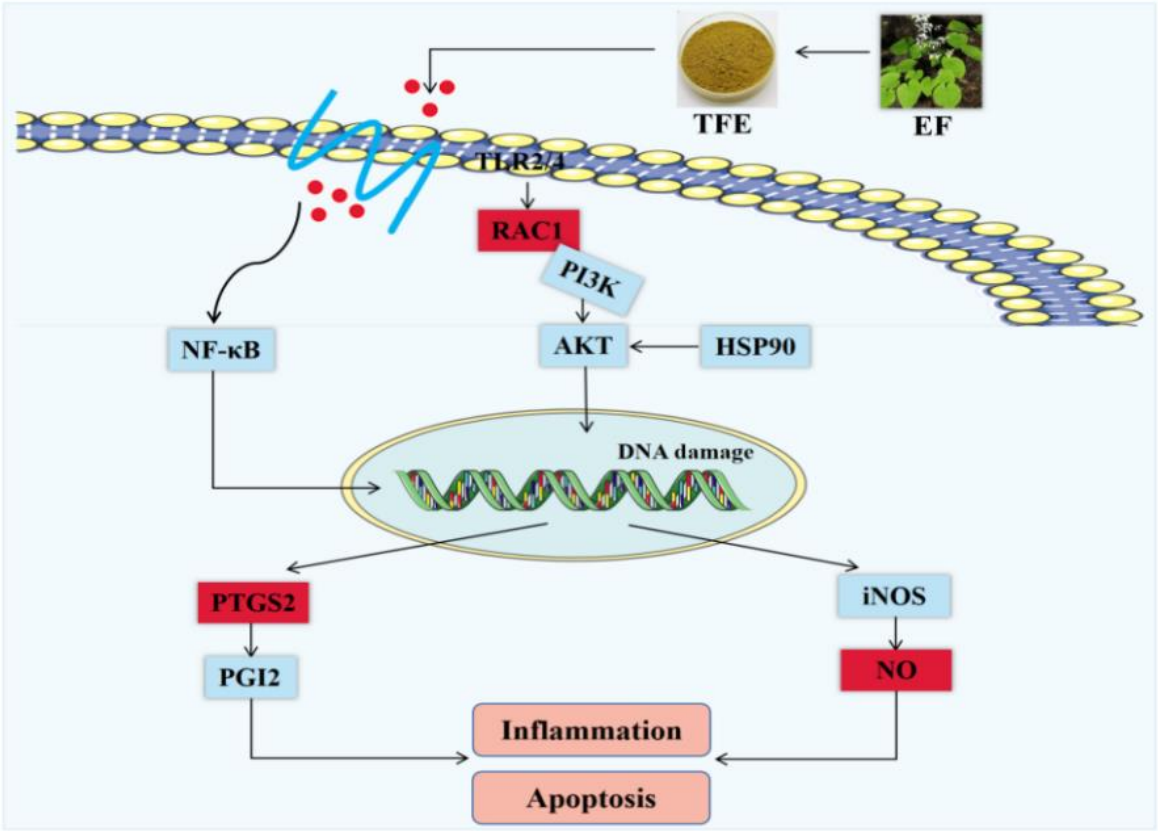

Figure 14 Mechanism of EF-induced DILI in HepaRG cells. The red square nodes represents the target proteins, and the black arrows represents interactions relationship.

Pathways involved in DILI

Analysis of the C-T-P network revealed that EF regulates 30 targets and 17 pathways. In GO analysis, these targets were associated with monomer metabolism, cell metabolism, catalytic activity and immune regulation, all of which are involved in the DILI process [3, 40–42]. KEGG pathway analysis showed that active compounds of EF regulated PI3K/Akt, NF-kB and VEGF signaling pathways.

Among the three pathways, the PI3K/Akt signaling pathway had the highest degree in the T-P network [43]. It has been reported that *E. adenophorum* induces the apoptosis of saanen goat hepatocytes via PI3K/Akt signaling pathways. Acetaminophen (APAP) induced acute DILI in rats by activating the PI3K/Akt signaling pathway. Elsewhere, treatment with Polygonum multiflorum induced L02 cell injuries and apoptosis by activating the PI3K/AKT signaling pathway. Besides, aflatoxin B2 induced DILI in broilers, through a mechanism involving Akt inhibition. These studies suggest that PI3K/Akt is involved in DILI initiation and promotion [44, 45]. Cellular experiments further revealed that EF altered the expressions of RAC1 as well as NOS3 and regulated the PI3K/AKT signaling pathway. The findings showed that CASP9, GSK3B, HSP90AA1, FLT3, NOS3, RAC1, RELA and MCL1 were involved in PI3K-Akt signaling pathways, suggesting that PI3K/Akt mediates the effects of EF on DILI.

The NF-kB signaling pathway is a downstream pathway of the PI3K-Akt signaling pathway. Overactivated NF-kB signaling pathway induces the release of inflammatory cytokines, leading to inflammation-induced damage of liver tissues [46–50]. Oxidative stress has been implicated in acetaminophen (APAP)-induced DILI, implying that oxidative stress can activate the NF-kB pathway to trigger inflammation, which enhances APAP-induced liver injury. In this study, PTGS2, RELA and ICAM1 were associated with the NF-kB signaling pathway. Cell experiments demonstrated that EF altered the expressions of PTGS2 and NF-kB signaling pathway. These findings indicate that the NF-kB signaling pathway plays an important role in EF-induced DILI.

Conclusion

We established that EF drives DILI through multiple compounds, targets, and signaling pathways, and that RAC1, PTGS2, and NOS3 are the key targets of EF-induced DILI. The PI3K/Akt and NF-kB signaling pathways mediate DILI by modulating oxidative stress, inflammation, and apoptosis. These findings form the basis for investigating the mechanisms underlying DILI induction by multiple EF-targets.

References

1. Leise MD, Poterucha JJ, Talwalkar JA. Drug-Induced Liver Injury. *Mayo Clin Proc*. 2014;89(1):95–106.
2. Chen M, Suzuki A, Borlak J, Andrade RJ, Lucena MI. Drug-induced liver injury: Interactions between drug properties and host factors. *J Hepatol*. 2015;63(2):503–514.
3. Woo KH, Lou YF. Progress in the pathogenesis and diagnosis of drug-induced liver injury. *Shanghai Med*. 2020;43(11):699-704.
4. Han D, Shinohara M, Ybanez MD, Saberi B, Kaplowitz N. Signal transduction pathways involved in drug-induced liver injury. *Handb Exp Pharmacol*. 2010;(196):267–310.
5. Stickel F, Patsenker E, Sehuppan D. Herbal hepatotoxicity. *J Hepatol*. 2005;43(5):901–910.
6. Kullak-Ublick GA, Andrade RJ, Merz M, et al. Drug-induced liver injury: recent advances in diagnosis and risk assessment. *Gut*. 2017;66(6):1154–1164.
7. Leung L, Kalgutkar AS, Obach RS. Metabolic activation in drug-induced liver injury. *Drug Metab Rev*. 2012;44(1):18–33.
8. William ML. Drug-induced Acute Liver Failure. *Clin Liver Dis*. 2013;17(4):575–586.
9. Xu JM. Investigation and analysis of multi-center hospitalized patients with acute drug-induced liver injury. *Chin J Gastroenterol*. 2007;27(7):439–442.
10. Kuijper IA, Yang H, Van De Water B, Beltman JB. Unraveling cellular pathways contributing to drug-induced liver injury by dynamical modeling. *Expert Opin Drug Metab Toxicol*. 2017;13(1):5–17.
11. Li YB, Meng FH, Lu XM, Li FM. Chemical composition of Epimedium epimedium. *Chin J Tradit Chin Med*. 2005;30(8):586–588.
12. Zhang DW, Cheng Y, Wang NL, Zhang JC, Yang MS, Yao XS. Effects of total flavonoids and flavonol glycosides from Epimedium koreanum Nakai on the proliferation and differentiation of primary osteoblasts. *Phytomedicine*. 2008;15(1–2):55–61.
13. Meng N, Kong K, Li SW. Research progress on phytochemical components and pharmacological activities of Epimedium. *J Northwest Flora*. 2010;30(5):1063–1073.
14. Zhao WJ, Wang L, Wang ZL, et al. Research progress on pharmacological action and clinical application of Epimedium. *Tradit Chin med inform*. 2016;33(2):105–108.
15. Xiong Y, Wu JR, Zhang CL. Progress in research on liver injury induced by Zhuanggu Joint Pill. *Central South Pharmacy*. 2019;17(12):2084–2087.
16. Li S, Wang XJ, Zhang W, et al. Analysis of adverse reactions/events in 39 cases of Xianling Gubao capsule. *Chin Pharm*. 2019;22(6):1068–1071.
17. Ding YN. Study on potential hepatotoxicity and drug interaction of xianling gubao capsule. Zhunyi: Zunyi Medical University; 2018.
18. Zhu CW, Wang HN, Zhang YL, Liu CH. Xianling Gubao Capsule causes liver injury. *Chin Hepatol*. 2018;23(12):1090–1093.
19. Wang D, Jia DX, Li ZZ, et al. Safety evaluation and risk control measures of Epimedium. *Chin J Chin Mater Med*. 2019;44(8):1715–1723.
20. Zhang L, Zhang JX, Fan QY, et al. Hepatoxicity of epimedii folium in rat model based on uniform design and regression analysis. *Chin J Exp Tradit Med Formulae*. 2018;24(6):189–197.
21. Lin HW, Jiang CX, Lu WQ, Piao SJ. Study on hepatocellular toxicity of xianling gubao tongfang extract. *Pharm Care Res*. 2020;20(2):98–101.
22. Zhang RT, Wu HN, Yu GH, Zhou YY, Jia XB, Feng L. Study on optimal effect components and signal pathways of Epimedium in disease prevention based on network pharmacology. *Chin J Tradit Chin Mater Med*. 2018;43(23):4709–4717.
23. Liu ZQ, Wang BL. Research progress in the selection of pharmacodynamic components and target prediction of traditional Chinese medicine network pharmacology. *Chin Tradit Patent med*. 2019;41(1):171–178.
24. Xie J, Gao S, Li L, Xu YL, Gao SM, Yu CQ. Research progress and application strategy of network pharmacology in the field of Traditional Chinese medicine. *Chin Tradit herbal Drugs*. 2019;50(10):2257–2265.
25. Yuan J, Hu J, He H, Zhang WJ. The progress of network pharmacology in the modernization of Traditional Chinese medicine. *Hainan Med*. 2020;31(20):2688–2691.
26. Ying QL, Yi C, Jia YF, Si QJ, Ping L, Fei L. Integrated network pharmacology and zebrafish model to investigate dual-effects components of Cistanche tubulosa for treating both Osteoporosis and Alzheimer's Disease. *J Ethnopharm*. 2020;254:112764.
27. Li YB, Meng FH, Lu XM, Li FM. Chemical composition of Epimedium epimedium. *Chin J Mater Med*. 2005;(8):586–588.
28. Ouyang HZ, He J. Progress in chemical composition analysis and pharmacokinetics of Epimedium. *J Tianjin Univ Tradit Chin Med*. 2019;38(3):219–227.
29. Navarro VJ, Barnhart H, Bonkovsky HL, et al. Liver injury from herbals and dietary supplements in the U. S Drug-Induced Liver Injury Network. *Hepatology*. 2014;6(4):1399–1408.
30. Garcia-Mediavilla V, Crespo I, Collado PS, et al. The anti-inflammatory flavones quercetin and kaempferol cause inhibition of inducible nitric oxide synthase, cyclooxygenase-2

and reactive C-protein, and down-regulation of the nuclear factor kappaB pathway in Chang Liver cells. *Eur J Pharmacol*. 2007;557(2–3):221–229.
31. Sun Y, Liu WZ, Liu T, Feng X, Yang N, Zhou HF. Signaling pathway of MAPK/ERK in cell proliferation, differentiation, migration, senescence and apoptosis. *J Recept Signal Transduct Res*. 2015;35(6):600–604.
32. Zhao Y, Zhang L, Wang Y, Mao H T, Cui ZY. Study on immune regulation of Icariin in vitro. *Chin Tradit herbal Drugs*. 1996;27(11):669–673.
33. Gao Y, Wang ZL, Tang JF, et al. New incompatible pair of TCM: Epimedii Folium combined with Psoraleae Fructus induces idiosyncratic hepatotoxicity under immunological stress conditions. *Front Med*. 2020;14(1):68–80.
34. Wu CS. Analysis of active components of Epimedium and study on its metabolism in vivo. Beijing: Peking Union Medical College; 2011.
35. Zhang L, Wang T, Zhao BS, et al. Effect of 2″-O-Rhamnosyl Icariside II, Baohuoside I and Baohuoside II in Herba Epimedii on Cytotoxicity Indices in HL-7702 and HepG2 Cells. *Molecules*. 2019;24(7):1263.
36. Li HY, Yang CP, Jin HT. Research progress on the mechanism of liver injury with commonly used drugs. *Chin J pharmacovigilance*. 2019;16(12):750–756.
37. Hu H, Han T, Zhuo M, et al. E levated COX-2 expression promotes angiogenesis through EGFR/p38-MAPK/Sp1-dependent signalling in pancreatic cancer. *Sci Rep*. 2017;7(1):470.
38. Cuadrado A, Martín-Moldes Z, Ye J, Lastres-Becker I. Transcription factors NRF2 and NF-κB are coordinated effectors of the Rho family, GTP-binding protein RAC1 during inflammation. *J Biol Chem*. 2014;289(22):15244–15258.
39. Pannen BH, Al-Adili F, Bauer M, et al. Role of endothelins and nitric oxide in hepatic reperfusion injury in rat. *Hepatology*. 1998;27(3):755–764.
40. Pan HL, Pan WJ, Chen CY, Deng ZH. Research progress of the effect of traditional Chinese medicine on liver toxicity. *J Clin Rational Drug Use*. 2020;13(27):179–181.
41. Jing X, Wu CQ, Wang QS, Wang QJ. Advances in the study of toxic pathways and molecular initiation events in drug liver injury. *Chin J New Drugs*. 2016;25(12):1348–1354.
42. Zhang Q, Lenardo MJ, Baltimore D. 30 Years of NF-κB: A Blossoming of Relevance to Human Pathobiology. *Cell*. 2017;168(1–2):37–57.
43. Huang C, Li J, Ma TT. PI3K/Akt signaling pathway and liver fibrosis. *Chin Pharmacol Bull*. 2011;27(8):1037–1041.
44. Reif S, Lang A, Lindquist JN, et al. The role of focal adhesion kinase-phosphatidylinositol 3-kinase akt signaling in hepatic stellate cell proliferation and type I collagen expression. *J Biol Chem*. 2003;278(10):8083–8090.
45. Wei L, Xiong H, Li W, Li B, Cheng Y. Upregulation of IL-6 expression in human salivary gland cell line by IL-17 via activation of p38 MAPK, ERK, PI3K/Akt, and NF-κB pathways. *J Oral Pathol Med*. 2018;47(9):847–855.
46. Li Q, Verma IM. NF-kappaB regulation in the immune system. *Nat Rev Immunol*. 2002;2(10):725–734.
47. Wulczyn FG, Krappmann D, Scheidereit C. The NF-kappa B/Rel and I kappa B gene families: mediators of immune response and inflammation. *J Mol Med (Berl)*. 1996;74(12):749–769.
48. Park SY, Bae YS, Ko MJ, et al. Comparison of anti-inflammatory potential of four different dibenzo cyclooctadiene lignans in microglia; action via activation of PKA and Nrf-2 signaling and inhibition of MAPK/STAT/NF-κB pathways. *Mol Nutr Food Res*. 2014;58(4):738–748.
49. Rakonczay ZJ, Jármay K, Kaszaki J, et al. NF-kappaB activation is detrimental in arginine-induced acute pancreatitis. *Free Radic Biol Med*. 2003;34(6):696–709.
50. Perkins ND. The Rel/NF-kappa B family: friend and foe. *Trends Biochem Sci*. 2000;25(9):434–440.